ACS APPLIED BIO MATERIALS Cite This: ACS Appl. Bio Mater. XXXX, XXX, XXX−XXX

Article

www.acsabm.org

Covalent Poly(lactic acid) Nanoparticles for the Sustained Delivery of Naloxone

Andrew J. Kassick,[†,‡] Heather N. Allen,[§] Saigopalakrishna S. Yerneni,[∥] Fathima Pary,[⊥] Marina Kovaliov,[†,‡] Cooper Cheng,[‡] Marco Pravetoni,[#] Nestor D. Tomycz,[‡] Donald M. Whiting,[‡] Toby L. Nelson,[⊥] Michael Feasel,[○] Phil G. Campbell,[∥,▽] Benedict Kolber,[§] and Saadyah Averick*[,†,‡]

[†]Neuroscience Disruptive Research Lab, Allegheny Health Network Research Institute, Allegheny General Hospital, Pittsburgh, Pennsylvania 15212, United States

[‡]Neuroscience Institute, Allegheny Health Network, Allegheny General Hospital, Pittsburgh, Pennsylvania 15212, United States

[§]Department of Biological Sciences and Chronic Pain Research Consortium, Duquesne University, Pittsburgh, Pennsylvania 15282, United States

[∥]Department of Biomedical Engineering, Carnegie Mellon University, Pittsburgh, Pennsylvania 15213, United States

[⊥]Department of Chemistry, Oklahoma State University, Stillwater, Oklahoma 74078, United States

[#]Department of Pharmacology, University of Minnesota Medical School Twin Cities, Minneapolis, Minnesota 55455, United States

[○]Chemical Biological Center, APG, U.S. Army Combat Capabilities Development Command, Edgewood, Maryland 21010, United States

[▽]Engineering and Engineering Research Accelerator, Carnegie Mellon University, Pittsburgh, Pennsylvania 15213, United States

Supporting Information

ABSTRACT: The opioid epidemic currently plaguing the United States has been exacerbated by an alarming rise in fatal overdoses as a result of the proliferated abuse of synthetic mu opioid receptor (MOR) agonists, such as fentanyl and its related analogues. Attempts to manage this crisis have focused primarily on widespread distribution of the clinically approved opioid reversal agent naloxone (Narcan); however, due to the intrinsic metabolic lability of naloxone, these measures have demonstrated limited effectiveness against synthetic opioid toxicity. This work reports a novel polymer-based strategy to create a long-acting formulation of naloxone with the potential to address this critical issue by utilizing covalent nanoparticle (*c*NP) drug delivery technology. Covalently loaded naloxone nanoparticles (Nal-*c*NPs) were prepared via the naloxone-initiated, ring-opening polymerization (ROP) of L-lactide in the presence of a bifunctional thiourea organocatalyst with subsequent precipitation of the resulting naloxone−poly(L-lactic acid) polymer. This protocol afforded well-defined nanoparticles possessing a drug loading of approximately 7% w/w. The resulting Nal-*c*NPs demonstrated excellent biocompatibility, while exhibiting sustained linear release kinetics *in vitro* and blocking the effects of high dose (10 mg/kg) acute morphine for up to 98 h in an *in vivo* rodent model of neuropathic pain.

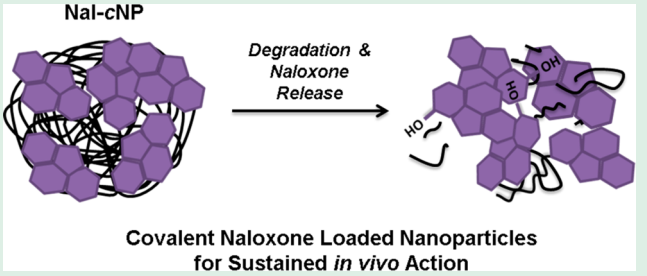

KEYWORDS: *naloxone, drug delivery, covalent nanoparticles, controlled release, ring-opening polymerization*

INTRODUCTION

For centuries, mu opioid receptor (MOR) agonists have been routinely employed by the medical community as an effective and reliable treatment for both moderate and severe pain. Despite their excellent therapeutic profiles, the heightened potential for addiction and abuse displayed by MOR agonists presents a serious liability.[1−5] This increased abuse potential has recently manifested in an unparalleled epidemic of opioid overdoses and deaths in the United States (U.S.) fueled by highly potent, synthetic MOR agonists, such as fentanyl (**1**) and its derivatives (Figure 1). According to a recent report by the Centers for Disease Control (CDC), the pervasive abuse of both prescription and illicit forms of synthetic opioids has been implicated in the exponential rise in opioid-related deaths observed in the U.S. since 2012.[6] Moreover, it has been estimated that, of the nearly 48 000 opioid-related mortalities reported in 2017, more than half have been attributed to synthetic opioid overdose.[6] Given this dramatic increase in

Received: May 3, 2019
Accepted: July 25, 2019
Published: July 25, 2019

DOI: 10.1021/acsabm.9b00380
ACS Appl. Bio Mater. XXXX, XXX, XXX−XXX

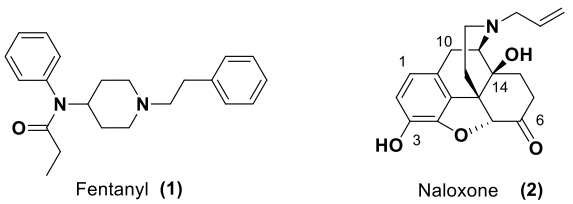

Figure 1. Fentanyl and naloxone (Narcan).

synthetic opioid-related deaths and the growing concern regarding the potential threat posed by these compounds to the general public, the opioid epidemic in the U.S. has recently been declared a national public health emergency.

While prompt administration of the MOR antagonist naloxone (**2**) has long been the primary means of treating an opioid overdose, this historical gold standard for opioid reversal has proven to be limited in its ability to effectively combat the deleterious effects of **1** and other highly potent synthetic opioids. This diminished efficacy can be explained by the rapid metabolism and clearance of naloxone via UGT2B7-mediated glucuronidation of the C3 phenol moiety coupled with the high potency and hydrophobicity possessed by synthetic MOR agonists. The hydrophobic nature of fentanyl-related analogues enables the facile absorption of these compounds into adipose tissue, thereby attenuating metabolism and effectively increasing their circulatory half-life.[7] Synthetic opioids can remain sequestered in tissues well after a therapeutic dose of naloxone has been eliminated from the body, resulting in a dangerous and potentially fatal condition known as renarcotization, in which a patient, despite being treated with naloxone, can experience the recurrence of toxicity from the slow permeation of residual synthetic opioids from adipose tissue.[8−11] As a result, the effective reversal of synthetic opioid overdose and prevention of renarcotization can require the administration of larger or multiple doses of naloxone, greatly complicating antidote delivery logistics. This phenomenon has been recently documented in several reports in patients treated with intravenous (IV), intramuscular (IM), or intranasal (IN) forms of naloxone.[9,11−14] Therefore, a critical need exists to develop new formulations of opioid reversal agents with improved pharmacokinetic profiles that are capable of providing longer-lasting antagonistic effects.

Given the challenges associated with identifying and optimizing entirely new chemical entities, we elected to incorporate the existing MOR antagonist, naloxone, into a delivery system capable of providing a sustained, therapeutic dose of drug in an attempt to more effectively treat the toxic effects of synthetic opioids. A promising strategy to achieve prolonged antidote infusion was anticipated through the application of biodegradable covalent nanoparticle (*c*NP) technology. We have previously demonstrated the feasibility of utilizing poly(lactic acid) (PLA)- and poly(lactide-*co*-glycolide) (PLGA)-derived *c*NPs as drug delivery systems in our exploration of extended release fentanyl-based analogues for improved pain management.[15] Our current approach to achieve sustained MOR antagonism is predicated on the analogous two-step covalent nanoparticle formulation strategy illustrated in Scheme 1. We speculated that the formation of covalently loaded naloxone nanoparticles (Nal-*c*NP) would occur by grafting commercially available L-lactide **3** from the phenolic hydroxyl moiety of naloxone, resulting in a low degree of polymerization (DP) naloxone−poly(L-lactic acid) polymer of type **4**. Subsequent precipitation of polymer **4** from an appropriate solvent system would then furnish well-defined polymeric nanoparticles with a high percent loading of naloxone, which, under physiological conditions, could degrade and release the desired opioid reversal agent. This method of covalent conjugation of drug to nanoparticle possesses several advantages over traditional, noncovalent nanoparticle delivery systems as it permits higher drug loadings and promotes batch-to-batch consistency in the preparation of NPs, while also avoiding the unwanted phenomenon of burst release,[16−19] which may precipitate withdrawal symptoms in opioid dependent individuals.[9,20] These advantages have been documented in several recent investigations comparing covalently conjugated NP formulations of fentanyl derivatives[15] and fluorescent Cy5 cyanine dyes[21] to their

Scheme 1. Schematic Representation of Covalent Naloxone Nanoparticle (Nal-*c*NP) Formation[a]

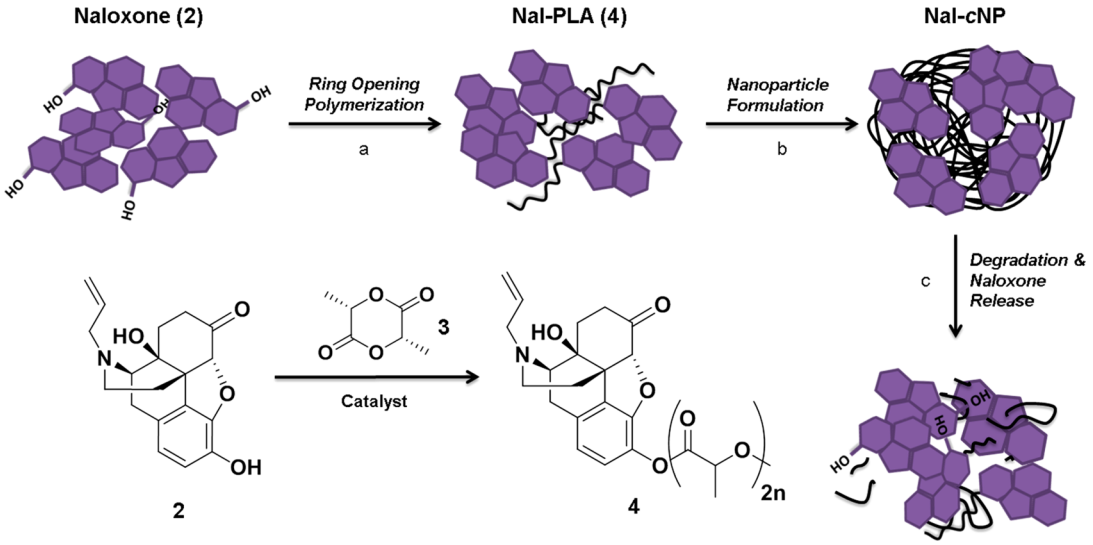

[a](a) Naloxone-initiated ring-opening polymerization of lactide **3** affords naloxone−poly(L-lactic acid) polymer **4**. (b) Polymer **4** is converted to the corresponding nanoparticles (Nal-*c*NPs). (c) Ester hydrolysis releases naloxone in a controlled manner.

DOI: 10.1021/acsabm.9b00380
ACS Appl. Bio Mater. XXXX, XXX, XXX−XXX

corresponding noncovalently encapsulated variants. Herein we report our results for the preparation and characterization of covalently loaded naloxone/PLA nanoparticles (Nal-*c*NPs) that demonstrate linear release kinetics *in vitro* and maintain an extended MOR blockade against the effects of high dose morphine vs free naloxone in a rodent model of neuropathic pain.

EXPERIMENTAL SECTION

Materials and Methods. Naloxone hydrochloride dihydrate was purchased from Sigma-Aldrich (St. Louis, MO) and subsequently converted to the corresponding free base (**2**) via acid−base extraction with saturated aqueous sodium bicarbonate ($NaHCO_3$). 1-[3,5-Bis(trifluoromethyl)phenyl]-3-[(1*R*,2*R*)-(−)-2-(dimethylamino) cyclohexyl]thiourea was obtained from Strem Chemicals, Inc. (Newburyport, MA). (3*S*)-*cis*-3,6-Dimethyl-1,4-dioxane-2,5-dione (L-lactide), anhydrous dichloromethane (CH_2Cl_2), dichloroethane (DCE), and toluene ($PhCH_3$) were purchased from Sigma-Aldrich (St. Louis, MO). Naloxone was dissolved in 0.9% saline at a dose of 10 mg/kg. Morphine sulfate, purchased from Sigma-Aldrich (St. Louis, MO), was dissolved in 0.9% saline at a dose of 10 mg/kg. Doses were determined based on previous publications.[22] Water was purified via a Millipore Synergy water purification system. All reagents and solvents were used as received unless otherwise noted. ^{1}H NMR spectra were measured in deuterochloroform ($CDCl_3$) or DMSO-d_6 on a Bruker Avance 500 MHz spectrometer. Chemical shifts are reported in ppm employing the residual solvent resonance as the internal standard ($CHCl_3$ δ 7.26 ppm, DMSO δ 2.50 ppm). UV−vis spectra were measured on a DeNovix DS-11 spectrophotometer using a 10 mm quartz cuvette. Gel permeation chromatography (GPC) was performed using a Waters GPC system equipped with a Waters 2410 refractive index detector. A Waters pump and a Styragel HR 3 column (7.8 × 300 mm) were used with THF as the mobile phase solvent. Separations were carried out at 35 °C with a flow rate of 1.0 mL/min. Polystyrene standards (M_n = 500−300 000 Da) were used for GPC system calibration. LC−MS analysis was performed on a Dionex Ultimate 3000 uHPLC system coupled to a Thermo Scientific TSQ Quantum Access MAX triple quadrupole mass spectrometer. Reverse-phase chromatographic separation was accomplished on an Agilent ZORBAX Eclipse Plus C18 column (3.5 μm, 100 mm × 4.6 mm) with acetonitrile (CH_3CN) and water (H_2O), modified with 0.1% formic acid, as the mobile phase solvents. The standard HPLC method consisted of a linear gradient from 1 to 95% CH_3CN over 5 min followed by a hold at 95% CH_3CN for 1 min and then a re-equilibration at 1% CH_3CN for 2.5 min. (total run time = 10 min, flow rate = 0.400 mL/min, injection volume = 10 μL, $T_{r\ naloxone}$ = ∼5.2 min).

Solvent-Free Synthesis of Naloxone−PLA Polymers. (3*S*)-*cis*-3,6-Dimethyl-1,4-dioxane-2,5-dione (**3**, 1.0 g, 6.94 mmol, 1 equiv) was added to an oven-dried 20 mL scintillation vial equipped with a magnetic stir bar under N_2. Lactide **3** was melted at 130 °C and then treated with a mixture of naloxone (0.227 g, 0.694 mmol, 10 mol %) and thiourea catalyst **5** (0.144 g, 0.347 mmol, 5 mol %). The reaction mixture was heated at 130 °C for 15 min to afford a viscous, yellow oil. Upon cooling to ambient temperature, the oil solidified and the bulk solid was dissolved in ∼10 mL of CH_2Cl_2. The polymer was purified by precipitation into 150 mL of cold MeOH by slow dropwise addition via syringe. The precipitate was collected via centrifugation at 4500 rpm for 30 min to furnish a pale yellow to off-white solid. After the supernatant liquid was decanted, the solid was subsequently washed with MeOH (15 mL) with centrifugation at 4500 rpm for 30 min (3 times). The precipitate was dried under a vacuum to afford 643 mg (52%) of the desired polymer as an off-white solid. ^{1}H NMR (500 MHz, $CDCl_3$): δ 6.85 (d, J = 8.3 Hz, 1H), 6.68 (d, J = 8.3 Hz, 1H), 5.87−5.77 (m, 1H), 5.19−5.13 (q, J = 7.1 Hz, 62 H), 4.67 (s, 1 H), 4.38−4.32 (m, 2 H), 3.21−3.09 (m, 3H), 3.06−2.96 (m, 2H), 2.65−2.56 (m, 2H), 2.40 (ddd, J = 5.1, 12.7, 12.7 Hz, 1H), 2.28 (ddd, J = 3.2, 3.2, 14.6 Hz, 1H), 2.13 (ddd, J = 3.8, 12.4, 12.4 Hz, 1H), 1.87 (ddd, J = 3.2, 5.0, 13.5 Hz, 1H), 1.58 (d, J = 7.1 Hz, 194H). GPC: M_n = 3000, M_w/M_n = 1.13.

Solution-Based Synthesis of Naloxone−PLA Polymers. Halogenated Solvents. An oven-dried microwave vial equipped with a magnetic stir bar was charged with L-lactide **3** (0.500 g, 3.47 mmol, 1 equiv) and purged with N_2 for 30 min, whereupon the lactide was dissolved in 4 mL of anhydrous solvent. A second oven-dried microwave vial was charged with naloxone (0.114 g, 0.347 mmol, 10 mol %) and thiourea catalyst (0.072 g, 0.173 mmol, 5 mol %) and purged with N_2 for 30 min. The solids were dissolved in 1 mL of anhydrous solvent. The solution of naloxone and catalyst was added to the lactide, and the reaction was maintained at the prescribed temperature for 24 h. The reaction was cooled to ambient temperature and then added to 75 mL of cold MeOH slowly dropwise via syringe. The resulting white suspension was centrifuged at 4000 rpm for 25 min (2 × 50 mL centrifuge tubes). The supernatant liquid was decanted, and the precipitate was resuspended in MeOH (25 mL each tube) and then centrifuged at 4000 rpm (repeated 3×). The resulting product was dried under a vacuum to obtain the desired polymer as a white solid (CH_2Cl_2 = 61 mg, 10%; DCE = 206 mg, 33%). For the $PhCH_3$ solvent, an oven-dried microwave vial equipped with a magnetic stir bar was charged with lactide (0.500 g, 3.47 mmol, 1 equiv) and purged with N_2 for 30 min, whereupon the lactide was suspended in 4 mL of anhydrous $PhCH_3$. A second oven-dried microwave vial was charged with naloxone (0.114 g, 0.347 mmol, 10 mol %) and thiourea catalyst (0.072 g, 0.173 mmol 5 mol %) and purged with N_2 for 30 min. The solids were suspended in 1 mL of anhydrous $PhCH_3$. The lactide was heated at 100 °C to dissolve and was then transferred to the suspension of naloxone and catalyst. The reaction mixture became a clear solution and was maintained at 100 °C for 24 h. The reaction was cooled to ambient temperature and then added to 75 mL of cold MeOH slowly dropwise via syringe. The resulting white suspension was centrifuged at 4000 rpm for 25 min (2 × 50 mL centrifuge tubes). The supernatant liquid was decanted, and the precipitate was resuspended in MeOH (25 mL each tube) and then centrifuged at 4000 rpm (repeated 3 times). The resulting product was dried under a vacuum to obtain 286 mg (47%) of a white solid. GPC: M_n = 2700, M_w/M_n = 1.10.

Preparation of Covalently Linked Naloxone−PLA Nanoparticles. A solution of the Nal-PLA polymer hybrid (40 mg) in 4 mL of CH_3CN was added slowly dropwise via syringe pump to a solution of 0.3% PVA in H_2O (30 mL) at a flow rate of 20 μL/min (0.02 mL/min) with rapid stirring. Upon completion of the addition, the resulting white, turbid mixture was maintained overnight at ambient temperature with rapid stirring. Nanoparticles were initially collected by centrifugation at 4500 rpm and then subsequently washed with H_2O (3 × 10 mL) with centrifugation at 4500 rpm for 30 min. The supernatant liquid was decanted, and the resultant precipitate was resuspended in about 10 mL of H_2O and lyophilized to yield 25 mg of a fluffy, white solid.

Covalent Nanoparticle Characterization. Size and ζ potential of the covalent nanoparticles were measured using a Particulate Systems NanoPlus3 dynamic light scattering (DLS) instrument and ζ potential analyzer equipped with a pH autotitrator. Solutions of covalent nanoparticles were prepared in ultrapure water at ∼0.1 mg/mL.

Transmission Electron Microscopy. A small drop of solution containing the sample was placed on a Formvar coated 300 mesh copper grid (Electron Microscopy Services, Hatfield, PA). After 30 s, the drop was removed by blotting with filter paper. The sample solution that remained on the grid was allowed to dry before inserting the grid into the microscope. The grids were viewed on a Hitachi H-7100 transmission electron microscope operating at 75 kV. Digital images were obtained using an AMT Advantage 10 CCD Camera System.

Naloxone Release Rate Determination. Nal-*c*NP (4.2 mg) was suspended in 4.2 mL of pH 7.4 phosphate buffered saline (1× PBS) with subsequent ultrasonication. The reaction vial was sealed then horizontally shaken in a GeneMate incubated shaker at 37 °C and 110

DOI: 10.1021/acsabm.9b00380
ACS Appl. Bio Mater. XXXX, XXX, XXX−XXX

Scheme 2. Organocatalyzed Naloxone-Initiated ROP of L-Lactide

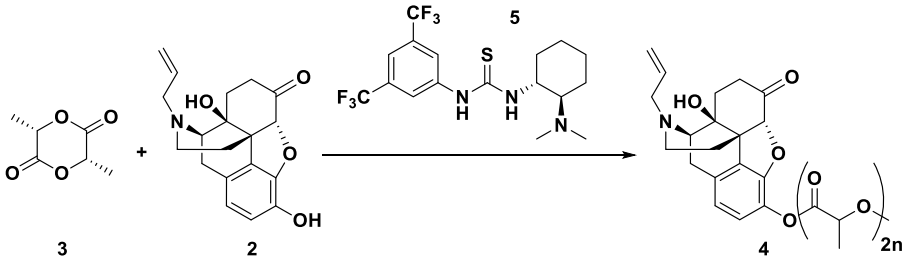

Table 1. Optimization of Organocatalyzed Naloxone-Initiated ROP of L-Lactide[c]

entry	solvent	temp (°C)	cat(mol %)	time (h)	conv (%)[a]	IE (%)[a]	M_n[b]	M_w/M_n[b]	DP[a]
a	neat	130	5	0.25	96	38	3000	1.13	64
b	CH_2Cl_2	rt	5	24	52	16	2200	1.06	66
c	DCE	80	5	24	85	22	2700	1.09	82
d	$PhCH_3$	100	5	24	98	27	2700	1.10	60

[a]Determined via ^{1}H NMR [b]Determined via GPC [c]Mole ratio of [lactide/naloxone] = 10:1

rpm. Aliquots (30 μL) were taken from the thoroughly mixed suspension at predetermined time intervals (up to 50 days) and centrifuged at 14 000 rpm for 5 min. Samples of the supernatant liquid (20 μL) were diluted with 500 μL of LC−MS grade H_2O and analyzed via LC−MS. Maximum naloxone *in vitro* release was determined by treating Nal-*c*NP (4.2 mg) with 4.2 mL of 1 M NaOH and incubating at 37 °C for 24 h. Given the fully degradable nature of PLA, complete hydrolysis and therefore complete naloxone release would be achieved under these conditions. *In vitro* controlled release was assessed via LC−MS by normalizing mass intensities taken from the extracted ion chromatogram (EIC) at each time point to maximum naloxone release and plotted as % naloxone release.

Cell Culture. Human embryonic kidney cells (HEK293; ATCC CRL-1573, Manassas, VA), murine embryonic fibroblast cells (NIH3T3; ATCC CRL-1658, Manassas, VA), and human keratinocytes (HaCaT; T0020001, Fisher Scientific, Waltham, MA) were grown and maintained in Dulbecco's modified Eagle media (DMEM; Gibco, Gaithersburg, MD) supplemented with 10% fetal bovine serum (Thermo Fisher Scientific, Waltham, MA) and 1% penicillin−streptomycin (Gibco, Gaithersburg, MD).

Cytotoxicity Assay. Cytotoxicity was assessed using a direct CyQUANT nucleic acid-sensitive fluorescence assay (Thermo Fisher Scientific, Waltham, MA, USA) according to the manufacturer's instructions. Briefly, 100 μL aliquots of cell suspension containing 1.25×10^3 cells/mL were plated in wells of a 96-well microplate (Corning Inc., Corning, NY, USA) and allowed to adhere for 6 h. PLA nanoparticles with varying concentrations were added to respective treatment wells and coincubated with cells for 72 h. Saponin (no. 84510, Sigma-Aldrich), 5 μg/mL, was used as a positive cytotoxicity control. After 72 h, cells were labeled with CyQUANT Direct and fluorescence intensities measured with a TECAN spectrophotometer reader (TECAN, Männedorf, Switzerland). Cytotoxicity was assessed by normalizing fluorescence intensities to the nontreatment control group and plotted as percent viability.

Animals. All mouse protocols were in accordance with the guidelines of the National Institute of Health and approved by the Animal Care and Use Committee of Duquesne University. Male and female C57Bl/6J mice underwent surgery for spared nerve injury at 9 weeks old. Animals were group housed with same-sex littermates after surgery and kept on a 12 h light/dark cycle from 7am to 7 pm with *ad libitum* access to food and water. Behavioral experimentation was performed during the light cycle when mice were 10−11 weeks of age. The experimenter was blinded to treatment until after all data was analyzed. Due to the large sample size (*n*) in this study, the experiment was performed in two cohorts of mice and all data was combined for analysis.

Spared Nerve Injury Surgery. Spared nerve injury was completed as previously described.[22] Briefly, mice were anesthetized with 3% isoflurane, and the fur over the left hindlimb was shaved with electric clippers. A small 1 cm incision was made in the skin parallel to the sciatic nerve, the biceps femoris muscle was moved aside, and the nerve was exposed. The tibial and common peroneal branches of the sciatic nerve were ligated with silk sutures and cut 2 mm distal to the ligatures. The sural nerve was left unmanipulated and intact. The skin was then closed with sutures over the surgical site, and mice recovered on a heating pad.

Behavioral Assay. Mechanical sensitivity was assayed with von Frey filaments to determine 50% withdrawal thresholds using the up/down method.[23,24] Animals were placed on wire mesh in individual Plexiglas boxes and allowed to habituate for 2 h prior to testing. Filaments ranging from 0.02 to 2.56 g were used to assay 50% withdrawal thresholds prior to SNI surgery (baseline). Seven days after surgery, mice were assessed for mechanical sensitivity again to confirm surgical success. An *a priori* threshold effect of SNI was set at 50%. In other words, animals exhibiting a less than 50% decrease in withdrawal threshold from the baseline were not included in the remainder of the study. Only 2 of 38 animals were excluded from the study based on this threshold. The remaining mice were divided into morphine or saline groups. On day 8 after SNI, intraperitoneal (IP) injections (100 μL) of either morphine (10 mg/kg) or saline vehicle were administered in a blinded fashion and mechanical sensitivity was assessed again at 2, 4, and 24 h post injection to demonstrate the time course of morphine efficacy in rodents with neuropathic pain. On day 10, 48 h following the first morphine/saline injection, animals again received IP injections (100 μL) of either morphine (10 mg/kg) or saline vehicle combined with a subcutaneous injection (10 μL/g) of free naloxone (10 mg/kg), Nal-*c*NP (1 mg/kg @ 7% w/w loading), or empty NP (*c*NP-empty), and mechanical sensitivity was assayed at 2 and 4 h post injection. Finally, morphine (10 mg/kg) or saline vehicle was injected again (100 μL) 1 day (day 11 post-SNI) and 3 days (day 14 post-SNI) after nanoparticle administration and mechanical sensitivity was assayed at 2 and 4 h time points following injection (corresponding to 26/28 and 98/100 h time points).

Statistical Analysis. Statistical analysis of all data was accomplished using GraphPad Prism 7 software. All data is shown as mean ± SEM. Von Frey behavioral data was analyzed using two-way Analysis of Variance (ANOVA) followed by Bonferroni post hoc tests. Data from the cytotoxicity assay was subjected to Analysis of Variance (ANOVA) followed by Tukey's post hoc test for multiple comparisons between treatment groups and the untreated control group. Statistical significance was defined as $p < 0.05$.

DOI: 10.1021/acsabm.9b00380
ACS Appl. Bio Mater. XXXX, XXX, XXX−XXX

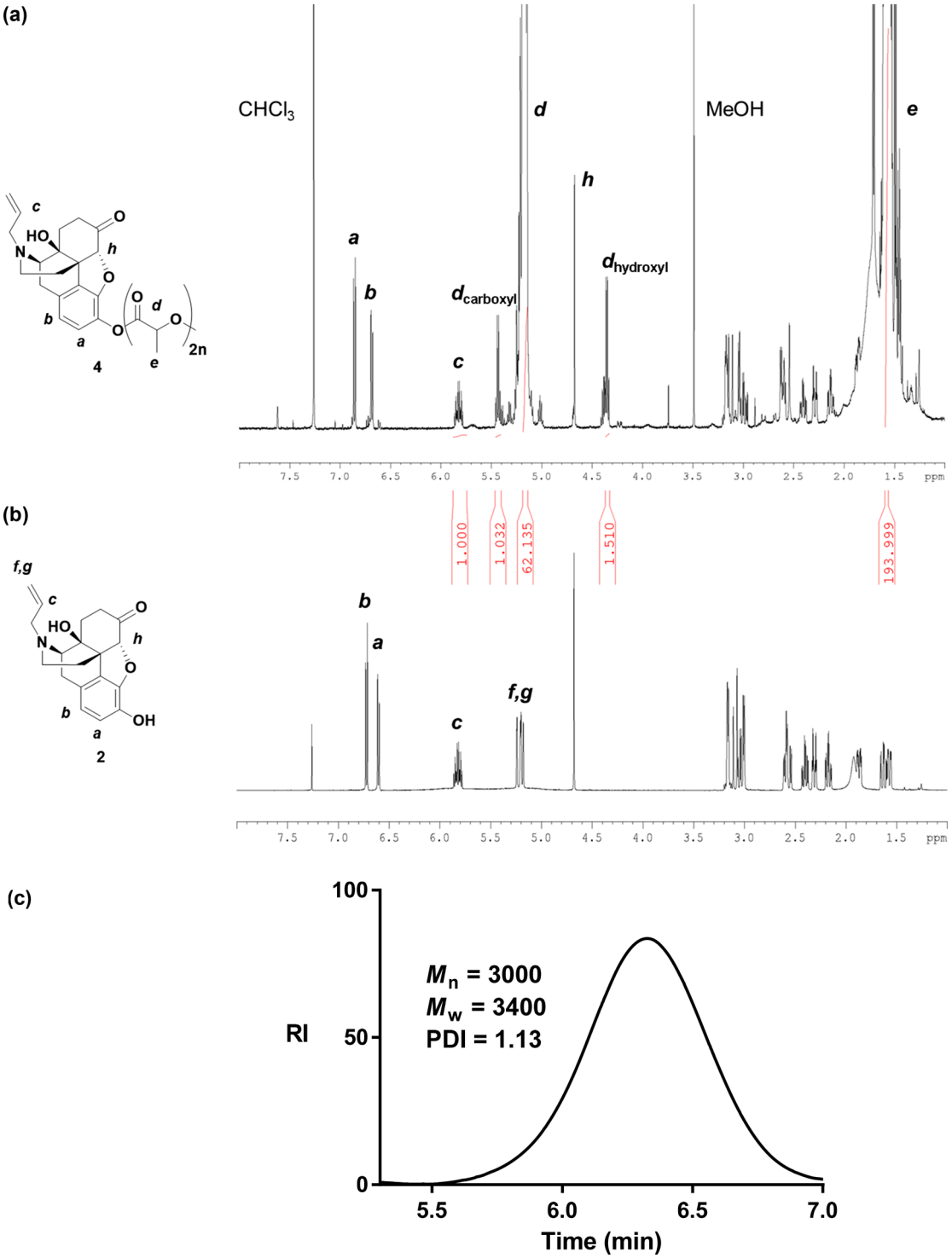

Figure 2. Characterization of naloxone functionalized PLA **4** prepared via organocatalyzed, solvent-free ROP of L-lactide: (a) ^{1}H NMR of Nal-PLA **4** in $CDCl_3$. Integration of vinylic CH vs lactic acid CH reveals DP of 64 (~7 wt % drug loading). (b) ^{1}H NMR of naloxone in $CDCl_3$. (c) GPC trace of Nal-PLA **4**.

RESULTS AND DISCUSSION

Synthesis of Naloxone–Polylactic Acid Polymer Hybrids. Aliphatic polyesters have traditionally been prepared via the catalytic ring-opening polymerization (ROP) of various lactide or lactone monomers using organometallic reagents.[25] Among the most widely employed metal-derived polymerization catalysts are tin-based species including the commercially available tin(II) 2-ethylhexanoate. While these compounds have been successfully utilized for the synthesis of polylactide polymers, their associated potential for toxicity remains a concern,[26−32] especially when generating materials to be employed in biomedical applications. As a result, we sought to identify a novel means of arriving at the requisite naloxone-initiated polymer **4** without relying on tin-based ROP catalysis.

DOI: 10.1021/acsabm.9b00380
ACS Appl. Bio Mater. XXXX, XXX, XXX−XXX

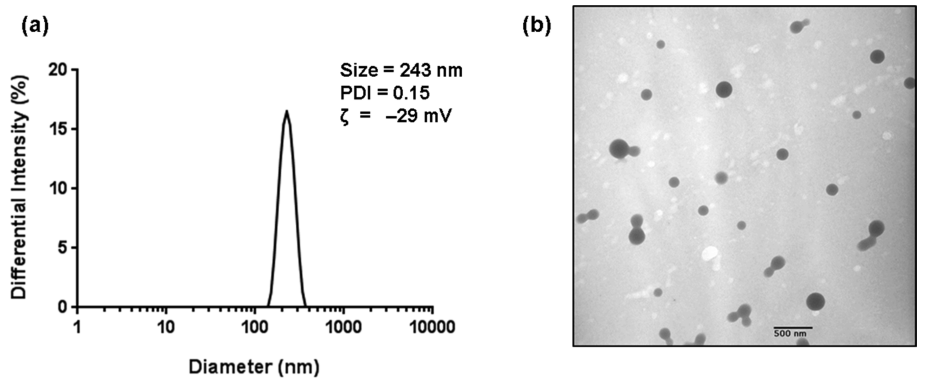

Figure 3. Characterization of covalently loaded Nalo-PLA NPs: (a) size distribution of Nal-*c*NP via DLS analysis and (b) transmission electron micrograph of Nal-*c*NP.

Table 2. Preparation and Characterization Summary for Nal-cNPs

entry	flow rate (μL/Min)	concentration[a] (mg/mL)	diameter[b] (nm)	PDI[b]
a	60	10	405	0.24
b	60	20	1314	0.64
c	20	10	243	0.15

[a]Concentration of Nal-PLA in CH_3CN prior to slow addition into 0.3% PVA (aq) [b]Average of 4 measurements

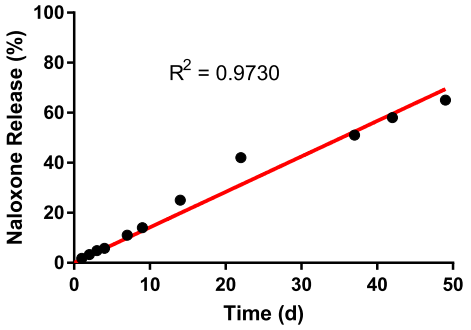

Figure 4. Cumulative release of naloxone from Nal-*c*NP in PBS buffer (pH 7.4). As indicated by the line of best fit (R^2 = 0.9730), there is a substantive linear release of naloxone from the Nal-*c*NPs.

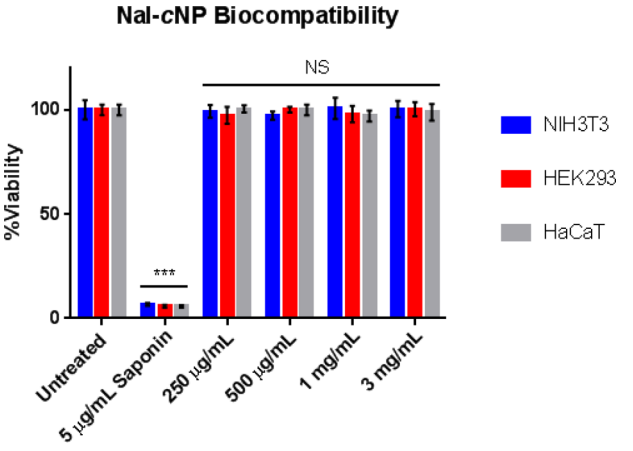

Figure 5. Biocompatibility assays illustrating the effect of 72 h treatment of cell lines with Nal-*c*NP versus the negative control (untreated) and positive cytotoxic control (Saponin). Data presented is the average of three replicates. NS = not significant compared to untreated, ***$p \leq 0.001$ compared to untreated.

Recent advances in the organocatalyzed ROP of cyclic esters have offered attractive alternatives to the standard Sn(II)-catalyzed polymerization conditions typically employed to arrive at the PLA-derived biopolymers of type **4** thus avoiding the use of potentially toxic heavy metals.[33,34] Hydrogen-bond-mediated catalyst systems derived from amidine or guanidine bases such as 1,8-diazabicyclo[5.4.0]undec-7-ene (DBU)[35−37] and 1,5,7-triazabicyclo[4.4.0]dec-5-ene (TBD)[36,38] or various thiourea/tertiary amine base cocatalysts[39−42] have been shown to grant unprecedented control over the molecular weight and polydispersity obtained in ROPs of lactone monomers with alcohol initiators. With regard to L-lactide **3**, literature examples have suggested that thiourea/amine cocatalyst systems are more effective than TBD for the ROP of lactide, allowing for the best control over the desired PLA polymer properties.[42] However, these organocatalytic polymerization reactions typically employ benzyl and primary alkyl alcohols as initiators and, to the best of our knowledge, no examples of organocatalyzed, phenol-initiated ROP reactions have been described. We therefore pursued a novel synthetic approach to the desired PLA polymer hybrid **4** via an organocatalyzed ROP of L-lactide from naloxone using a thiourea/tertiary amine catalyst system (Scheme 2).

Our studies to determine optimal reaction conditions for the thiourea/tertiary amine-catalyzed ROP of lactide **3** are summarized in Table 1. In order to achieve a higher drug loading of naloxone, a low DP polymer (DP ∼ 20) was targeted by selecting a 10:1 molar ratio of lactide monomer to initiator in the ROP reactions. Bifunctional thiourea catalyst **5**, originally developed by Takemoto and co-workers,[43,44] was selected for these screening experiments as it offered the convenience of containing both thiourea and tertiary amine functional groups required for monomer and nucleophile activation, respectively (Scheme 2). Our catalyst loading (5 mol %) reflected standard loadings employed for ROP reactions with thiourea **5** reported in the literature. We initially examined the effectiveness of **5** under solvent-free conditions but also explored the possibility of carrying out the polymerizations under milder solvent-based reaction conditions. Under solvent-free conditions, a mixture of solid thiourea **5** (5 mol %) and naloxone (10 mol %) was added in one portion to premelted L-lactide at 130 °C. For the solvent-based reactions, L-lactide **3** was dissolved in solvent (∼0.7 M in lactide) and a solution of naloxone and catalyst **5** was added to start the polymerization; however, a reverse

DOI: 10.1021/acsabm.9b00380
ACS Appl. Bio Mater. XXXX, XXX, XXX−XXX

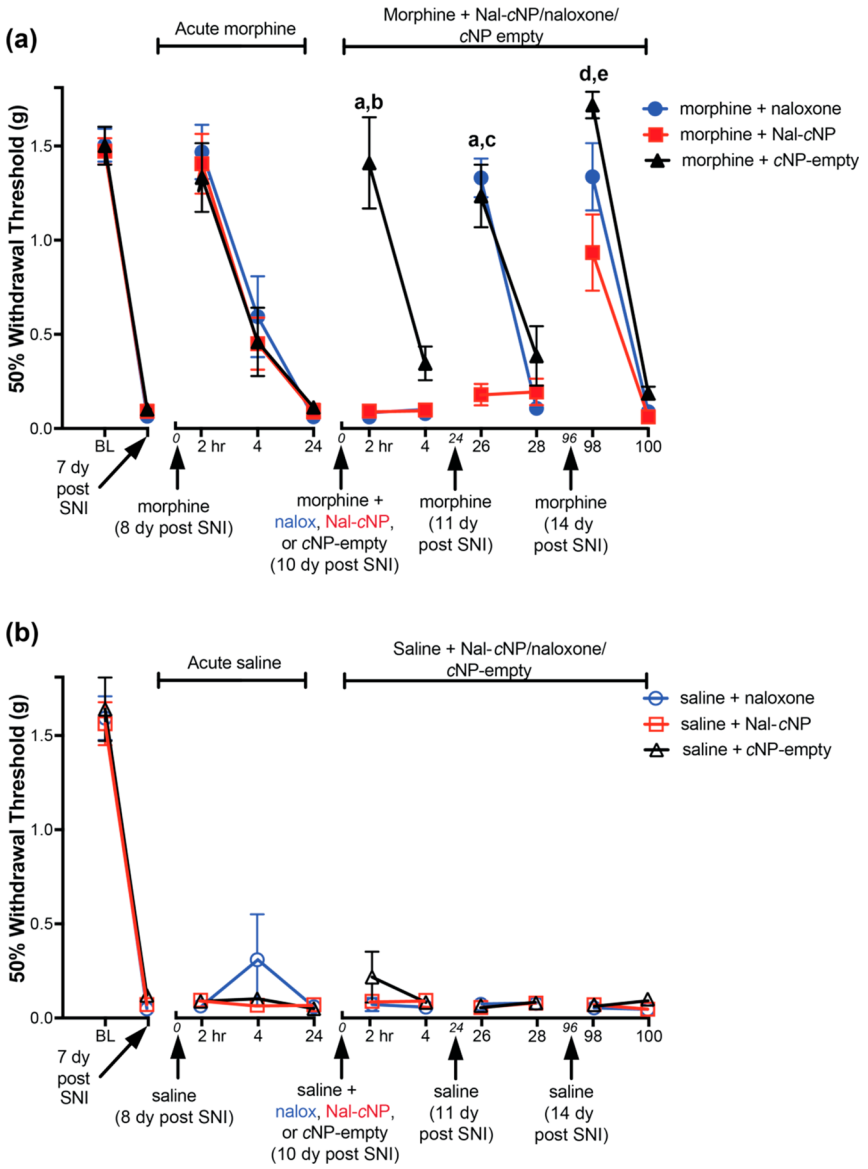

Figure 6. *In vivo* efficacy of Nal-*c*NP and free naloxone in a spared nerve injury (SNI) mouse model treated with morphine (a) or saline (b). Bonferroni post hoc tests (a) represent significance ($p < 0.001$) between *c*NP-empty and Nal-*c*NP, (b) represent significance ($p < 0.001$) between *c*NP-empty and naloxone, (c) represent significance ($p < 0.001$) between naloxone and Nal-*c*NP, (d) represent significance ($p < 0.05$) between naloxone and Nal-*c*NP, and e represent significance ($p < 0.01$) between *c*NP-empty and Nal-*c*NP; $n = 6$ per group.

addition of lactide to naloxone and thiourea at 100 °C was required in the case of toluene solvent due to the poor solubility of the initiator and catalyst. Reactions were conducted for the prescribed times (Table 1), and the resulting polymers were purified via precipitation into cold MeOH. HPLC traces of the purified polymer demonstrated no free catalyst or monomer was present after purification (Figure S1).

As documented in Table 1, solvent-free conditions (entry a) resulted in the rapid and complete conversion of L-lactide to the desired polymer **4** within 15 min and afforded excellent control over the molecular weight and polydispersity (M_n = 3000, M_w/M_n = 1.13) as determined by GPC analysis (Figure 2c). Comparable results were obtained for the solvent-based reaction employing toluene (entry d), wherein complete conversion to the desired polymer **4** was observed after 24 h at 100 °C (M_n = 2700, M_w/M_n = 1.10). Attempts at polymerization under milder temperatures with solvents like CH_2Cl_2 and DCE (entries b and c) resulted in lower conversions, indicating the need for elevated temperatures to achieve the desired reactivity. Given its operationally simple reaction setup, faster reaction times, and avoidance of potentially toxic solvents, we opted to utilize the solvent-free route for the production of larger batches of Nal-PLA **4** for further studies.

The polymer structure and degree of polymerization (DP) for Nal-PLA prepared via both solvent-free and solution-based methods were confirmed by ^{1}H NMR analysis (Figure 2 and Figures S2–S4), and the corresponding drug loading of naloxone was determined using standard polymer molecular weight analysis techniques (eqs S3–S5).[45] ^{1}H NMR spectra recorded in both $CDCl_3$ (Figures 2a,b) and DMSO-d_6 (Figures S2a,b) revealed a significant downfield shift in the aryl ring proton resonances of naloxone (***a*** and ***b***) following ROP, suggesting that the polymerization of lactide occurred from the C3 phenol, a result consistent with the characteristic

DOI: 10.1021/acsabm.9b00380
ACS Appl. Bio Mater. XXXX, XXX, XXX–XXX

deshielding effects of an adjacent ester functionality. Further support for this assignment was obtained upon inspection of the ^{1}H NMR spectra of naloxone and Nal-PLA **4** in DMSO-d_6 where the disappearance of the phenolic proton resonance ***i*** from the Nal-PLA spectrum can be clearly noted (Figures S2a,b). ^{1}H NMR analysis in DMSO-d_6 is necessary in this instance due to the rapid exchangeability of the phenolic proton in $CDCl_3$. Selective incorporation of lactide from the phenolic hydroxyl is also demonstrated through the lack of appreciable changes in chemical shift exhibited by the protons adjacent to the C14 hydroxyl moiety (***m*** and ***t***), as well as the presence of the tertiary alcohol proton (***s***) (Figures S3a,b and S4a,b). This chemoselective acylation of the phenolic hydroxyl moiety of naloxone in the presence of its free C14 tertiary alcohol has also been well documented in the literature, thus permitting the present polymer structure to be assigned by analogy.[46,47] Polymer DPs, presented in Table 1, were based on the ratio of integrals between the methine protons of the polymer chain of Nal-PLA (***d***), including carboxylic and hydroxylic end groups ($\boldsymbol{d}_{\text{carboxyl}}$, $\boldsymbol{d}_{\text{hydroxyl}}$), and the vinylic proton resonance of the naloxone chain end (***c***) (Figure 2a). From these values, it could be determined that drug loadings of approximately 7 wt % were achieved for both solvent-free and $PhCH_3$-based preparation methods (eqs S4 and S5, respectively). Further confirmation of the naloxone content of our Nal-*c*NPs was obtained via UV−vis spectrophotometric analysis of a 0.3 mg/mL solution of Nal-PLA **4** (DP = 64, Figure S5). The naloxone concentration of the sample was determined to be 0.0197 mg/mL or a 6.6% w/w naloxone loading, which was in excellent agreement with our initial ^{1}H NMR estimation. It should be noted that, while high conversions of lactide to Nal-PLA were generally observed at elevated temperatures, ^{1}H NMR analysis of the crude product mixtures showed that reactions proceeded with incomplete initiation of polymer growth from naloxone. The resulting initiator efficiencies (IE) for the reaction conditions investigated ranged from 16 to 38% (Table 1 and eq S2). Further optimization of IE could be used to arrive at enhanced DPs and, as a result, polymers bearing higher naloxone loadings.

Nanoparticle Preparation and Characterization. Having arrived at a method to synthesize naloxone terminal PLA polymers possessing suitable drug loadings, attention was focused on the preparation of the desired covalently functionalized NPs. Nal-PLA polymer **4** was converted to the corresponding *c*NPs using a previously described nanoprecipitation method.[15,48] Nal-PLA polymer **4** in acetonitrile (10 mg/mL) was slowly added via syringe pump (20 μL/min) to a stirred 0.3% aqueous solution of poly(vinyl alcohol) (PVA). The resulting *c*NPs were collected by centrifugation, then purified, and lyophilized to afford the desired Nal-*c*NPs.

Subsequent characterization of Nal-*c*NP was achieved via dynamic light scattering (DLS), ζ potential, and transmission electron microscopy (TEM). DLS measurements revealed the formation of well-defined particles that possessed an average diameter of 243 nm and a narrow, monomodal size distribution with polydispersity of 0.15 (Figure 3a). Nal-*c*NP also exhibited a strong, negative ζ potential value (ζ = −29 mV) consistent with the presence of lactic acid chain ends and their observed stability and lack of particle aggregation upon dispersion in water.[49−51] These results were confirmed by TEM morphological analysis, which provided images of well-dispersed, spherical Nal-*c*NPs lacking any visible surface cracks or voids (Figure 3b).

We attempted to prepare additional Nal-*c*NPs possessing different sizes by varying the parameters of polymer addition rate and concentration as depicted in Table 2. An increase in hydrodynamic diameter was observed when the infusion rate of polymer was increased (entry a), while maintaining the original polymer concentration (10 mg/mL). Larger particles were obtained by adding a more concentrated polymer mixture (entry b) for precipitation into 0.3% aqueous PVA. Although DLS analysis revealed the ability to form larger diameter Nal-*c*NPs, these particles were not selected for further evaluation due to their broader molecular weight distributions as characterized by their higher PDIs (0.235 and 0.635, respectively). It has been recently demonstrated in the literature that the sustained release properties of NPs are impacted by their corresponding molecular weight distributions.[52,53] Given that more disperse particles were typically found to produce a greater variability in release kinetics, we elected to pursue our low PDI *c*NPs (entry c) due to their more homogeneous particle population size characteristics to ensure a more uniform release of drug.

***In Vitro* Naloxone Release Studies.** Controlled release studies were performed to evaluate the ability of Nal-*c*NP to provide a linear, sustained dose of naloxone. *In vitro* naloxone release rates were determined by incubation of Nal-*c*NP at 37 °C in 1× phosphate buffered saline (pH 7.4) over the course of 7 weeks with concomitant monitoring of the appearance of naloxone via LC−MS. Data points were normalized to maximum naloxone release obtained via base-mediated *c*NP hydrolysis in the presence of 1 M NaOH at 37 °C for 24 h. As shown in Figure 4, our preliminary *in vitro* release studies illustrate a prolonged, linear release of naloxone demonstrating that Nal-*c*NP is a suitable vehicle for the sustained delivery of naloxone as it avoids undesired burst release kinetics. While the observed drug release was very slow, requiring approximately 7 weeks to achieve the cumulative release of 65% naloxone, it was anticipated that Nal-*c*NP would exhibit faster rates of drug release *in vivo* due to exposure to endogenous hydrolytic enzymes not present in the *in vitro* experiment, a known phenomenon for drug-eluting nanoparticles.[54]

***In Vitro* Biocompatibility Assay.** Our assessment of Nal-*c*NP for potential cytotoxic activity against multiple cell lines is presented in Figure 5. Human embryonic kidney cells (HEK293), murine embryonic fibroblasts (NIH3T3), and human keratinocytes (HaCaT) were evaluated as they represent tissues that could be exposed to *c*NPs following a subcutaneous or intramuscular injection, the preferred routes of *c*NP administration. To determine biocompatibility, cell treatment groups were incubated for 72 h in the presence of various concentrations of Nal-*c*NP and then compared to both untreated cells and an additional grouping incubated with 5 μg/mL of the cytotoxic agent, saponin, as a positive control. Gratifyingly, Nal-*c*NP showed no significant influence on cell viability across the tested concentration range for all three cell lines (250 μg/mL to 3 mg/mL), clearly demonstrating its excellent biocompatibility.

***In Vivo* Efficacy.** We measured the *in vivo* efficacy of Nal-*c*NP by blocking the analgesic effects of free morphine in a mouse model of neuropathic injury. In this experiment, animals exhibited mechanical hypersensitivity associated with a spared nerve injury (SNI). We sought to (1) block this hypersensitivity acutely with morphine and (2) evaluate whether Nal-*c*NP (7% w/w; 1 mg/kg) could in turn block the analgesic effects of morphine compared to free naloxone

DOI: 10.1021/acsabm.9b00380
ACS Appl. Bio Mater. XXXX, XXX, XXX−XXX

(10 mg/kg). SNI caused a significant decrease in mechanical threshold (two-way RM ANOVA, effect of SNI $p < 0.0001$; Bonferoni post hoc test $P < 0.0001$ compared to baseline (BL) Figure 6a). On day 8 after SNI, mice were treated with morphine IP (10 mg/kg; 8 day post-SNI). Morphine significantly reduced this mechanical hypersensitivity for up to 4 h (two-way RM ANOVA, main effect of treatment $p < 0.0001$, Bonferroni post hoc tests, 2 h $p < 0.0001$, 4 h $p < 0.0001$, 24 h $p > 0.05$ compared to day 7 post-SNI time point). On day 10 after SNI, mice were treated again with morphine (10 mg/kg IP) along with either Nal-*c*NP, *c*NP-empty, or free naloxone (subcutaneous). Nal-*c*NP (1 mg/kg, 7% naloxone loading, $n = 6$) was as effective as free naloxone (10 mg/kg, $n = 6$) at maintaining acute MOR blockade against the effects of high dose morphine in the SNI mouse model for 2 h (Figure 6a) (two-way RM ANOVA, main effect of treatment $p < 0.0001$, main effect of time $p < 0.0001$, Bonferroni post hoc tests, 2 h $p < 0.001$, 4 h $p > 0.05$). On day 11 after SNI, mice were treated again IP with morphine. At this time, only Nal-*c*NP was found to effectively block the analgesic effects of morphine treatment compared to free naloxone or *c*NP-empty, demonstrating the full wash out of free naloxone (Bonferroni post hoc test 26 h $P < 0.001$). Finally, on day 14 after SNI, mice were treated for the final time with IP morphine (96 h time point since naloxone treatment). Nal-*c*NP continued to reduce the effect of this morphine (Bonferroni post hoc test $P < 0.01$ compared to 98 h *c*NP-empty and $P < 0.05$ compared to 98 h free naloxone). This effect of Nal-*c*NP for up to 98 h after administration is more than 4 times longer than free naloxone. All of the above experiments with morphine analgesia were also simultaneously completed in mice treated IP with saline prior to Nal-*c*NP, free naloxone, or *c*NP-empty. Neither Nal-*c*NP nor *c*NP-empty had any significant effect in control animals (Figure 6b) (two-way RM ANOVA, main effect of treatment $p = 0.3556$).

Because the effect of Nal-*c*NP was still significant against morphine at 98 h, the present experiment does not allow for determination of the precise *in vivo* time course for Nal-*c*NP. Future studies will include additional time points after 98 h as well as time points between 28 and 96 h to assess the full length of Nal-*c*NP's efficacy against morphine. A longer-lasting opioid, such as PolyMorphine,[55] should be used in future studies as it shows analgesic effects in mice with neuropathic pain for up to 24 h[22] compared to the 4 h efficacy of free morphine seen in the present study. The extended analgesic-like effects of PolyMorphine would allow a more detailed assessment of Nal-*c*NP's efficacy against morphine by allowing inclusion of more time points without requiring more injections, therefore reducing the risk of morphine-induced hypersensitivity that comes with repeated morphine injections. Comparison of intramuscularly administered Nal-*c*NP, as opposed to subcutaneous administration, should also be investigated as a means of increasing the delivered dose of naloxone, as should size and naloxone percent of the nanoparticle.

CONCLUSION

In the present study, we have developed an effective drug delivery system for the extended release of naloxone utilizing covalently loaded polylactic acid (PLA) nanoparticles. Biodegradable PLA-based *c*NP precursors were synthesized using naloxone-initiated ROP of L-lactide under solvent-free conditions in the presence of a bifunctional thiourea organocatalyst. The resultant polymers were characterized by GPC analysis and ^{1}H NMR spectroscopy demonstrating good control over molecular weight and a high drug loading of naloxone (7% w/w). Subsequent conversion to the corresponding *c*NPs was accomplished by employing a previously reported nanoprecipitation protocol that yielded well-defined, spherical particles as confirmed by DLS and TEM analysis. The Nal-*c*NP particles showed no signs of *in vitro* cytotoxicity against multiple cell lines (up to 3 mg/mL), demonstrating their excellent biocompatibility. Controlled release studies demonstrated a linear, sustained release of naloxone without the undesired phenomenon of burst release. *In vivo* studies in SNI mice revealed the enhanced capability of Nal-*c*NP to promote superior levels of extended MOR receptor blockade against high dose morphine relative to free naloxone (up to 98 h), suggesting that our functionalized *c*NPs have the potential to dramatically improve the ability of naloxone to combat the toxic effects of fentanyl and other synthetic opioids. Additional *in vitro* and *in vivo* studies toward the further optimization of Nal-*c*NP for synthetic opioid reversal are currently underway and will be reported in due course.

ASSOCIATED CONTENT

Supporting Information

The Supporting Information is available free of charge on the ACS Publications website at DOI: 10.1021/acsabm.9b00380.

Experimental calculations, characterization data, NMR spectra, HPLC traces, and UV−vis spectra (PDF)

AUTHOR INFORMATION

Corresponding Author

*E-mail: Saadyah.Averick@ahn.org. Tel: +1-412-359-4943.

ORCID

Marco Pravetoni: 0000-0003-1036-0184
Toby L. Nelson: 0000-0001-5549-6072
Michael Feasel: 0000-0001-7029-2764
Saadyah Averick: 0000-0003-4775-2317

Notes

The authors declare no competing financial interest.

ACKNOWLEDGMENTS

We gratefully acknowledge The Army Research Office (award no. 68271-CH) Young Investigator Program (W911NF-17-1-0015) and the Neuroscience Institute at AHN for funding. NMR measurements and instrumentation at CMU, which was partially supported by NSF (CHE-0130903 and CHE-1039870), the National Institutes of Health (UL1TR001857) and through a Pain Research Challenge Grant (to B.J.K. and H.N.A.), were supported by the Clinical and Translational Science Institute at the University of Pittsburgh.

REFERENCES

(1) Contet, C.; Kieffer, B. L.; Befort, K. Mu Opioid Receptor: A Gateway to Drug Addiction. *Curr. Opin. Neurobiol.* **2004**, *14*, 370−378.

(2) Le Merrer, J.; Becker, J. A. J.; Befort, K.; Kieffer, B. L. Reward Processing by the Opioid System in the Brain. *Physiol. Rev.* **2009**, *89*, 1379−1412.

(3) Pattinson, K. T. S. Opioids and the Control of Respiration. *Br. J. Anaesth.* **2008**, *100*, 747−758.

(4) Negus, S. S.; Freeman, K. B. Abuse Potential of Biased Mu Opioid Receptor Agonists. *Trends Pharmacol. Sci.* **2018**, *39*, 916−919.

DOI: 10.1021/acsabm.9b00380
ACS Appl. Bio Mater. XXXX, XXX, XXX−XXX

(5) Pasternak, G. W. Mu Opioid Pharmacology: 40 Years to the Promised Land. *Adv. Pharmacol.* **2018**, *82*, 261−291.
(6) National Institute on Drug Abuse. https://www.drugabuse.gov/related-topics/trends-statistics/overdose-death-rates.
(7) Peng, P. W. H.; Sandler, A. N. A Review of the Use of Fentanyl Analgesia in the Management of Acute Pain in Adults. *Anesthesiology* **1999**, *90*, 576−599.
(8) Dahan, A.; Aarts, L.; Smith, T. W. Incidence, Reversal, and Prevention of Opioid-Induced Respiratory Depression. *Anesthesiology* **2010**, *112*, 226−238.
(9) Zuckerman, M.; Weisberg, S. N.; Boyer, E. W. Pitfalls of Intranasal Naloxone. *Prehosp. Emerg. Care* **2014**, *18*, 550−554.
(10) van der Schier, R.; Roozekrans, M.; van Velzen, M.; Dahan, A.; Niesters, M. Opioid-Induced Respiratory Depression: Reversal by Non-Opioid Drugs. *F1000Prime Rep.* **2014**, *6*, 79−86.
(11) Sutter, M. E.; Gerona, R. R.; Davis, M. T.; Roche, B. M.; Colby, D. K.; Chenoweth, J. A.; Adams, A. J.; Owen, K. P.; Ford, J. B.; Black, H. B.; Albertson, T. E. Fatal Fentanyl: One Pill Can Kill. *Acad. Emerg. Med.* **2017**, *24*, 106−113.
(12) Wermeling, D. P. Review of Naloxone Safety for Opioid Overdose: Practical Considerations for New Technology and Expanded Public Access. *Ther. Adv. Drug Saf.* **2015**, *6*, 20−31.
(13) Rzasa Lynn, R.; Galinkin, J. L. Naloxone Dosage for Opioid Reversal: Current Evidence and Clinical Implications. *Ther. Adv. Drug Saf.* **2018**, *9*, 63−88.
(14) Kelly, A. M.; Kerr, D.; Dietze, P.; Patrick, I.; Walker, T.; Koutsogiannis, Z. Randomised Trial of Intranasal Versus Intramuscular Naloxone in Prehospital Treatment for Suspected Opioid Overdose. *Med. J. Aust.* **2005**, *182*, 24−27.
(15) Kovaliov, M.; Li, S.; Korkmaz, E.; Cohen-Karni, D.; Tomycz, N.; Ozdoganlar, O. B.; Averick, S. Extended-Release of Opioids Using Fentanyl-Based Polymeric Nanoparticles for Enhanced Pain Management. *RSC Adv.* **2017**, *7*, 47904−47912.
(16) Du, A. W.; Stenzel, M. H. Drug Carriers for the Delivery of Therapeutic Peptides. *Biomacromolecules* **2014**, *15*, 1097−1114.
(17) Tong, R.; Cheng, J. Ring-Opening Polymerization-Mediated Controlled Formulation of Polylactide−Drug Nanoparticles. *J. Am. Chem. Soc.* **2009**, *131*, 4744−4754.
(18) Huang, X.; Brazel, C. S. On the Importance and Mechanisms of Burst Release in Matrix-Controlled Drug Delivery Systems. *J. Controlled Release* **2001**, *73*, 121−136.
(19) Kamaly, N.; Yameen, B.; Wu, J.; Farokhzad, O. C. Degradable Controlled-Release Polymers and Polymeric Nanoparticles: Mechanisms of Controlling Drug Release. *Chem. Rev.* **2016**, *116*, 2602−2663.
(20) Clarke, S. F. J. Naloxone in Opioid Poisoning: Walking the Tightrope. *Emerg. Med. J.* **2005**, *22*, 612−616.
(21) Chaney, E. J.; Tang, L.; Tong, R.; Cheng, J.; Boppart, S. A. Lymphatic Biodistribution of Polylactide Nanoparticles. *Mol. Imaging* **2010**, *9*, 153−162.
(22) Lax, N. C.; Chen, R.; Leep, S. R.; Uhrich, K. E.; Yu, L.; Kolber, B. J. Polymorphine Provides Extended Analgesic-Like Effects in Mice with Spared Nerve Injury. *Mol. Pain* **2017**, *13*, 174480691774347.
(23) Dixon, W. J. Efficient Analysis of Experimental Observations. *Annu. Rev. Pharmacol. Toxicol.* **1980**, *20*, 441−462.
(24) Chaplan, S. R.; Bach, F. W.; Pogrel, J. W.; Chung, J. M.; Yaksh, T. L. Quantitative Assessment of Tactile Allodynia in the Rat Paw. *J. Neurosci. Methods* **1994**, *53*, 55−63.
(25) Dechy-Cabaret, O.; Martin-Vaca, B.; Bourissou, D. Controlled Ring-Opening Polymerization of Lactide and Glycolide. *Chem. Rev.* **2004**, *104*, 6147−6176.
(26) Viau, C. M.; Guecheva, T. N.; Sousa, F. G.; Pungartnik, C.; Brendel, M.; Saffi, J.; Henriques, J. A. P. Sncl2-Induced DNA Damage and Repair Inhibition of Mms-Caused Lesions in V79 Chinese Hamster Fibroblasts. *Arch. Toxicol.* **2009**, *83*, 769−775.
(27) Yamada, T.; Jung, D.-Y.; Sawada, R.; Tsuchiya, T. Intracerebral Microinjection of Stannous 2-Ethylhexanoate Affects Dopamine Turnover in Cerebral Cortex and Locomotor Activity in Rats. *J. Biomed. Mater. Res., Part B* **2008**, *87B*, 381−386.
(28) Platel, R.; Hodgson, L.; Williams, C. Biocompatible Initiators for Lactide Polymerization. *Polym. Rev.* **2008**, *48*, 11−63.
(29) Guo, J.; Haquette, P.; Martin, J.; Salim, K.; Thomas, C. M. Replacing Tin in Lactide Polymerization: Design of Highly Active Germanium-Based Catalysts. *Angew. Chem., Int. Ed.* **2013**, *52*, 13584−13587.
(30) Roe, F. J. C.; Boyland, E.; Millican, K. Effects of Oral Administration of Two Tin Compounds to Rats over Prolonged Periods. *Food Cosmet. Toxicol.* **1965**, *3*, 277−280.
(31) de Groot, A. P.; Feron, V. J.; Til, H. P. Short-Term Toxicity Studies on Some Salts and Oxides of Tin in Rats. *Food Cosmet. Toxicol.* **1973**, *11*, 19−30.
(32) Tanzi, M. C.; Verderio, P.; Lampugnani, M. G.; Resnati, M.; Dejana, E.; Sturani, E. Cytotoxicity of Some Catalysts Commonly Used in the Synthesis of Copolymers for Biomedical Use. *J. Mater. Sci.: Mater. Med.* **1994**, *5*, 393−396.
(33) Dove, A. P. Organic Catalysis for Ring-Opening Polymerization. *ACS Macro Lett.* **2012**, *1*, 1409−1412.
(34) Kiesewetter, M. K.; Shin, E. J.; Hedrick, J. L.; Waymouth, R. M. Organocatalysis: Opportunities and Challenges for Polymer Synthesis. *Macromolecules* **2010**, *43*, 2093−2107.
(35) Brown, H. A.; De Crisci, A. G.; Hedrick, J. L.; Waymouth, R. M. Amidine-Mediated Zwitterionic Polymerization of Lactide. *ACS Macro Lett.* **2012**, *1*, 1113−1115.
(36) Lohmeijer, B. G. G.; Pratt, R. C.; Leibfarth, F.; Logan, J. W.; Long, D. A.; Dove, A. P.; Nederberg, F.; Choi, J.; Wade, C.; Waymouth, R. M.; Hedrick, J. L. Guanidine and Amidine Organocatalysts for Ring-Opening Polymerization of Cyclic Esters. *Macromolecules* **2006**, *39*, 8574−8583.
(37) Coady, D. J.; Fukushima, K.; Horn, H. W.; Rice, J. E.; Hedrick, J. L. Catalytic Insights into Acid/Base Conjugates: Highly Selective Bifunctional Catalysts for the Ring-Opening Polymerization of Lactide. *Chem. Commun.* **2011**, *47*, 3105.
(38) Pratt, R. C.; Lohmeijer, B. G.; Long, D. A.; Waymouth, R. M.; Hedrick, J. L. Triazabicyclodecene: A Simple Bifunctional Organocatalyst for Acyl Transfer and Ring-Opening Polymerization of Cyclic Esters. *J. Am. Chem. Soc.* **2006**, *128*, 4556−4557.
(39) Dove, A. P.; Pratt, R. C.; Lohmeijer, B. G. G.; Waymouth, R. M.; Hedrick, J. L. Thiourea-Based Bifunctional Organocatalysis: Supramolecular Recognition for Living Polymerization. *J. Am. Chem. Soc.* **2005**, *127*, 13798−13799.
(40) Spink, S. S.; Kazakov, O. I.; Kiesewetter, E. T.; Kiesewetter, M. K. Rate Accelerated Organocatalytic Ring-Opening Polymerization of L-Lactide Via the Application of a Bis(Thiourea) H-Bond Donating Cocatalyst. *Macromolecules* **2015**, *48*, 6127−6131.
(41) Kazakov, O. I.; Kiesewetter, M. K. Cocatalyst Binding Effects in Organocatalytic Ring-Opening Polymerization of L-Lactide. *Macromolecules* **2015**, *48*, 6121−6126.
(42) Pothupitiya, J. U.; Dharmaratne, N. U.; Jouaneh, T. M. M.; Fastnacht, K. V.; Coderre, D. N.; Kiesewetter, M. K. H-Bonding Organocatalysts for the Living, Solvent-Free Ring-Opening Polymerization of Lactones: Toward an All-Lactones, All-Conditions Approach. *Macromolecules* **2017**, *50*, 8948−8954.
(43) Okino, T.; Hoashi, Y.; Takemoto, Y. Enantioselective Michael Reaction of Malonates to Nitroolefins Catalyzed by Bifunctional Organocatalysts. *J. Am. Chem. Soc.* **2003**, *125*, 12672−12673.
(44) Okino, T.; Nakamura, S.; Furukawa, T.; Takemoto, Y. Enantioselective Aza-Henry Reaction Catalyzed by a Bifunctional Organocatalyst. *Org. Lett.* **2004**, *6*, 625−627.
(45) Izunobi, J. U.; Higginbotham, C. L. Polymer Molecular Weight Analysis By1h Nmr Spectroscopy. *J. Chem. Educ.* **2011**, *88*, 1098−1104.
(46) Ukrainets, I. V.; Tkach, A. A.; Gorokhova, O. V.; Turov, A. V.; Linsky, I. V. Studies of 3-O-Acyl Derivatives of Naloxone as Its Potential Prodrugs. *Chem. Heterocycl. Compd.* **2009**, *45*, 405−416.
(47) Béni, S.; Tóth, G.; Noszál, B.; Hosztafi, S. Preparation of Benzoate Esters of Morphine and Its Derivatives. *Monatsh. Chem.* **2012**, *143*, 1431−1440.

DOI: 10.1021/acsabm.9b00380
ACS Appl. Bio Mater. XXXX, XXX, XXX−XXX

(48) Sanna, V.; Roggio, A.; Posadino, A.; Cossu, A.; Marceddu, S.; Mariani, A.; Alzari, V.; Uzzau, S.; Pintus, G.; Sechi, M. Novel Docetaxel-Loaded Nanoparticles Based on Poly(Lactide-Co-Caprolactone) and Poly(Lactide-Co-Glycolide-Co-Caprolactone) for Prostate Cancer Treatment: Formulation, Characterization, and Cytotoxicity Studies. *Nanoscale Res. Lett.* **2011**, *6*, 260.
(49) Agrawal, Y. K.; Patel, V. Nanosuspension: An Approach to Enhance Solubility of Drugs. *J. Adv. Pharm. Technol. Res.* **2011**, *2*, 81.
(50) Bhattacharjee, S. Dls and Zeta Potential − What They Are and What They Are Not? *J. Controlled Release* **2016**, *235*, 337−351.
(51) Yildirim, I.; Yildirim, T.; Kalden, D.; Festag, G.; Fritz, N.; Weber, C.; Schubert, S.; Westerhausen, M.; Schubert, U. S. Retinol Initiated Poly(Lactide)S: Stability Upon Polymerization and Nanoparticle Preparation. *Polym. Chem.* **2017**, *8*, 4378−4387.
(52) Dutta, D.; Salifu, M.; Sirianni, R. W.; Stabenfeldt, S. E. Tailoring Sub-Micron Plga Particle Release Profiles Via Centrifugal Fractioning. *J. Biomed. Mater. Res., Part A* **2016**, *104*, 688−696.
(53) Chen, W.; Palazzo, A.; Hennink, W. E.; Kok, R. J. Effect of Particle Size on Drug Loading and Release Kinetics of Gefitinib-Loaded Plga Microspheres. *Mol. Pharmaceutics* **2017**, *14*, 459−467.
(54) Athanasiou, K. Sterilization, Toxicity, Biocompatibility and Clinical Applications of Polylactic Acid/ Polyglycolic Acid Copolymers. *Biomaterials* **1996**, *17*, 93−102.
(55) Rosario-Meléndez, R.; Harris, C. L.; Delgado-Rivera, R.; Yu, L.; Uhrich, K. E. Polymorphine: An Innovative Biodegradable Polymer Drug for Extended Pain Relief. *J. Controlled Release* **2012**, *162*, 538−544.

DOI: 10.1021/acsabm.9b00380
ACS Appl. Bio Mater. XXXX, XXX, XXX−XXX